

Semi-organised structures and turbulence in the atmospheric convection

I. Rogachevskii^{1,2*} and N. Kleeorin^{1,3†}

¹*Department of Mechanical Engineering, Ben-Gurion University of the Negev, Beer-Sheva 8410530, Israel*

²*Nordita, Stockholm University and KTH Royal Institute of Technology, 10691 Stockholm, Sweden*

³*Institute of Continuous Media Mechanics, Korolyov str. 1, Perm 614013, Russia*

(Dated: November 27, 2023)

The atmospheric convective boundary layer (CBL) consists in three basic parts: (i) the surface layer unstably stratified and dominated by small-scale turbulence of very complex nature; (ii) the CBL core dominated by the energy-, momentum- and mass-transport of semi-organised structures (large-scale circulations), with a small contribution from small-scale turbulence produced by local structural shears; (iii) turbulent entrainment layer at the upper boundary, characterised by essentially stable stratification with negative (downward) turbulent flux of potential temperature. The energy- and flux budget (EFB) theory developed previously for atmospheric stably-stratified turbulence and the surface layer in atmospheric convective turbulence is extended to the CBL core using budget equations for turbulent energies and turbulent fluxes of buoyancy and momentum. For the CBL core, we determine global turbulent characteristics (averaged over the entire volume of the semi-organised structure) as well as kinetic and thermal energies of the semi-organised structures as the functions of the aspect ratio of the semi-organised structure and the scale separation parameter between the vertical size of the structures and the integral scale of turbulence. The obtained theoretical relationships are potentially useful in modelling applications in the atmospheric convective boundary-layer.

I. INTRODUCTION

Conventional theory of turbulence and methods of calculation of turbulent transport coefficients are based on the following classical paradigm [1–11]. Turbulent flow represents a superposition of the two types of motion: fully organised mean flow and fully chaotic turbulence produced, e.g., by the mean-flow velocity shears. Turbulence comprises an ensemble of chaotic motions (turbulent eddies) of different scales characterised by the forward energy cascade from larger to smaller eddies. The spectrum of turbulence has an inertial range characterised by the energy flux towards smaller eddies with constant energy dissipation rate. The energy flux is balanced by the viscous dissipation at the smallest eddies at the viscous range of scales.

Accordingly, the mean flow is treated deterministically, while turbulence is described statistically. The local characteristics of turbulence (in particular, turbulent fluxes that appear in the Reynolds-averaged equations) are controlled by local features of the mean flow. The turbulent flux of any transporting property is proportional to the mean gradient of the property multiplied by appropriate turbulent-exchange coefficient. This concept of down-gradient turbulent transport reduces the turbulence-closure problem to determining the above exchange coefficients: eddy viscosity K_M , eddy diffusivity K_D and turbulent heat conductivity K_H that, in turn, are assumed proportional to the product of turbulent kinetic energy E_K and turbulent time scale t_T . The above turbulence paradigm and the concept of down-gradient

transport have been formulated by Kolmogorov [12–15] for the shear-generated turbulence in neutrally stratified flows, and have proven applicable to a wide range of neutrally and weakly stably or unstably stratified flows.

However, there is increasing evidence of their poor applicability to both strongly stable stratification and strongly unstable stratification [16–27]. The present paper is devoted to atmospheric convective boundary layer (CBL), which involve besides the mean flow and Kolmogorov’s turbulence, the two additional types of motion disregarded in the conventional theory:

- small-scale buoyancy-driven vertical plumes, which exhibit inverse energy transfer, namely, merge to form larger and larger plumes instead of breaking down and feeding kinetic energy of horizontal velocity fluctuations, as it should be in the case of the forward cascade [8, 28–31];
- large-scale semi-organised convective structures (energetically supplied by merging plums), which embrace the entire CBL, and perform non-local transports irrespective of mean gradients of transporting properties [32–40].

We recall that the CBL in the atmosphere develops against strongly stable stratification in the free flow. This leads to formation of comparatively thin, stably stratified turbulent entrainment layer at the CBL upper boundary. The turbulent entrainment layer separates CBL from the free atmospheric flow and acts similarly to the upper lid in laboratory experiments, causing development of semi-organised structures: large-scale convective cells (the cloud cells) in the shear-free CBL (analogous to large-scale circulations in laboratory experiments) and large-scale convective rolls (the cloud streets) in the sheared CBL [41–43]. The convective semi-organised structures

* gary@bgu.ac.il; <http://www.bgu.ac.il/~gary>

† nat@bgu.ac.il

disturb the CBL-free flow interface, which leads to exciting internal gravity waves in the free atmospheric flow and pumping the energy out of CBL [8, 44, 45]. Accounting for the above processes, it is convenient to divide CBL into the three basic parts:

- shallow surface layer strongly unstably stratified and dominated by vertical transport due to the small-scale three-dimensional turbulence produced by both mean-wind shears and structural convective-wind shears of semi-organised structures, and strongly anisotropic buoyancy-driven merging-plum turbulence;
- deep CBL core with preferable vertical transport due to the semi-organised structures and small contribution from three-dimensional turbulence produced by local shears of the semi-organised structures, and very small vertical gradient of the mean potential temperature;
- shallow turbulent entrainment layer at the CBL upper boundary with strong stable stratification dominated by turbulent transport and the downward turbulent flux of potential temperature.

Observations in the atmospheric CBL, laboratory experiments and large-eddy simulation (LES) confirm that convective structures principally differ from turbulent eddies. The characteristic scales of the semi-organised structures are much larger than the integral turbulence scale and their life-times are much longer than the largest turbulent time scales [40–43]. In the shear-free atmospheric CBL, the semi-organised structures (the cloud cells) are similar to Bernard cells. They consist of narrow uprising flows surrounded by wide downdraughts, embrace the entire CBL (up to 1–3 km height), and include pronounced convergence flows towards the cell axes in the near-surface layer, as well as divergence flows at the CBL upper boundary. In the sheared CBL, the semi-organised structures (the cloud streets) have the form of rolls stretched along the mean wind. Various features in the atmospheric convective turbulence have been studied theoretically and numerically [31, 37–39, 46–55], and in the field experiments [30, 37, 47, 56–58], see reviews [9, 59–61], and references therein.

Deterministic treatment of semi-organised convective structures as distinct from turbulence treated statistically has been employed to derive non-local convective heat/mass-transfer law for the shear-free CBL [32, 37, 62–64]. Interesting features of convective turbulence now attributed to merging-plume mechanism implying inverse energy transfer from smaller to larger plumes were found long ago [8, 28–31]. The ideas that the shear-produced turbulence interacts with convective semi-organised structures in the same way as with usual mean flow have been used in a number of studies [38, 39, 64].

In the present paper we focus on physical processes in the CBL core and extend the energy- and flux budget

(EFB) turbulence closure theory developed previously for atmospheric stably-stratified turbulence [24, 44, 45, 65–67], turbulent transport of passive scalar [68] and the surface layers in atmospheric convective turbulence [69], to convective turbulence in the CBL core in shear-free convection with very weak mean wind.

The EFB theory for the stably stratified turbulence explains existence of strong turbulence produced by large-scale shear for any stratification [24, 44, 45, 65–67]. The physics related to self-maintaining of a stably stratified turbulence for any stratification is caused by the following. The increase of the buoyancy due to an enhancement of the vertical gradient of the mean potential temperature results in a conversion of turbulent kinetic energy (TKE) into turbulent potential energy (TPE). This decreases the negative down-gradient vertical turbulent flux of potential temperature by a positive non-gradient turbulent flux of potential temperature originated from enhanced TPE. This mechanism of the self-control feedback decreases the buoyancy and maintain stably stratified turbulence for any stratification [11, 68, 69] in agreement with wide experimental evidence [16–20, 22, 23, 25, 27, 70].

The EFB theory for the surface layers in atmospheric convective turbulence [69] describes a smooth transition between a stably-stratified turbulence and a convective turbulence, providing analytical expressions for the vertical profiles for all turbulent characteristics in the entire surface layer including TKE, the intensity of turbulent potential temperature fluctuations, the vertical turbulent fluxes of momentum and buoyancy (proportional to potential temperature), the integral turbulence scale, the turbulence anisotropy, the turbulent Prandtl number and the flux Richardson number. The obtained analytical vertical profiles describe also the transition range between the lower and upper parts of the surface layer.

The EFB theory for the CBL core developed in the present study, is based on the three-fold decomposition: mean flow, semi-organised structures and small-scale turbulence, in combination with analytical description of convective semi-organised structures in the shear-free CBL. We find the global turbulent characteristics (averaged over the entire volume of the semi-organised structure) and kinetic and thermal energies of the semi-organised structures, which depend on the aspect ratio of the semi-organised structure and scale separation parameter between the vertical size of the structures and the integral scale of turbulence. The obtained theoretical relationships are potentially useful in modelling applications in the atmospheric convective boundary-layer.

This paper is organized as follows. In Sec. II we discuss turbulent flux of potential temperature and its effect on formation of semi-organised structures. In this section we derive expressions for the velocity and potential temperature of convective semi-organised structures. In Sec. III we study turbulence in the CBL core, starting with budget equations for turbulent energies and turbulence fluxes of potential temperature and momentum (Sec. III A), and formulate main assumptions for the en-

ergy and flux budget turbulence closure theory for convective turbulence (Sec. III B). In the framework of this theory, we derive expressions for the global characteristics of convective turbulence and semi-organised structures (Sec. III C). In Sec. IV we consider a transition from the convective surface layer to the CBL core, where we perform a matching between the solutions obtained for the convective surface layer and the CBL core. Finally, in Sec. V we discuss the obtained results and draw conclusions.

II. TURBULENT FLUX OF POTENTIAL TEMPERATURE AND SEMI-ORGANISED STRUCTURES

The convective boundary layer involves three principally different types of motion:

- regular plain-parallel mean flow homogeneous in the horizontal plain (coordinates x, y), but heterogeneous in the vertical (coordinate z);
- vertically and horizontally heterogeneous long-lived CBL-scale semi-organised convective structures; and
- small-scale turbulence.

We use capital letters with superscript (m) to denote the mean-flow fields of wind: $\overline{\mathbf{U}}^{(m)} = (\overline{U}_x^{(m)}, \overline{U}_y^{(m)}, \overline{U}_z^{(m)})$, pressure $\overline{P}^{(m)}$ and potential temperature $\overline{\Theta}^{(m)}$; capital letters with superscript (s) to denote the semi-organised structure fields, $\overline{\mathbf{U}}^{(s)} = (\overline{U}_x^{(s)}, \overline{U}_y^{(s)}, \overline{U}_z^{(s)})$, and $\overline{P}^{(s)}, \overline{\Theta}^{(s)}$; lower-case letters to denote turbulent fields: \mathbf{u}, p and θ ; and just capital letters to denote actual (total) fields, e.g., the total velocity is $\mathbf{U} = \overline{\mathbf{U}}^{(m)} + \overline{\mathbf{U}}^{(s)} + \mathbf{u}$, the total pressure is $P = \overline{P}^{(m)} + \overline{P}^{(s)} + p$ and the total potential temperature is $\Theta = \overline{\Theta}^{(m)} + \overline{\Theta}^{(s)} + \theta$. In the present study, we consider a shear-free convection with negligible mean flow field, $\overline{\mathbf{U}}^{(m)} = 0$, but with a non-zero vertical gradient of the mean potential temperature $\nabla_z \overline{\Theta}^{(m)} \neq 0$.

Turbulent fluxes of potential temperature and momentum are defined as $\mathbf{F} = \langle \mathbf{u} \theta \rangle$ and $\tau_{ij} = \langle u_i u_j \rangle$, respectively, where angle brackets denote ensemble averaging. For the sake of definiteness, we restrict our consideration to dry atmosphere, so that buoyancy is proportional to the potential temperature $\Theta = T(P_*/P)^{1-\gamma^{-1}}$, where T is the fluid temperature with the reference value T_* , P is the fluid pressure with the reference value P_* and $\gamma = c_p/c_v$ is the specific heat ratio. The familiar down-gradient approximation of the turbulent fluxes of potential temperature and momentum reads: $\mathbf{F} = -K_H \nabla \overline{\Theta}$ and $\tau_{ij} = -K_M (\nabla_i \overline{U}_j + \nabla_j \overline{U}_i)$, where $\overline{\Theta} = \overline{\Theta}^{(m)} + \overline{\Theta}^{(s)}$, $\overline{\mathbf{U}} = \overline{\mathbf{U}}^{(s)}$, K_H and K_M are turbulent heat conductivity

and turbulent viscosity traditionally treated as scalars [1, 2, 59].

On the other hand, there are long-lived CBL-scale semi-organised convective structures and the velocity field inside large-scale convective structures is strongly nonuniform. These nonuniform motions can produce anisotropic velocity fluctuations which can contribute to the turbulent flux of potential temperature. In particular, the classical turbulent flux of potential temperature, $\mathbf{F} = -K_H \nabla \overline{\Theta}$, does not take into account the contribution from anisotropic velocity fluctuations.

A. Turbulent flux of potential temperature

The contribution to the turbulent flux of potential temperature from anisotropic velocity fluctuations plays a crucial role in formation of large-scale semi-organised structures in turbulent convection. Indeed, the turbulent flux of potential temperature \mathbf{F} which takes into account anisotropic velocity fluctuations reads [38, 39]:

$$\mathbf{F} = \mathbf{F}^* - \frac{8 t_T}{9} \left[\alpha \mathbf{F}_z^* \operatorname{div} \overline{\mathbf{U}}_h^{(s)} - \frac{2\alpha + 3}{10} \overline{\mathbf{W}}^{(s)} \times \mathbf{F}_z^* \right], \quad (1)$$

where $\mathbf{F}^* = -K_H \nabla \overline{\Theta}^{(m)}$ is the classical background turbulent flux of potential temperature in the absence of nonuniform large-scale flows, α is the degree of thermal anisotropy that characterises the form of plumes and is defined by Eq. (20), t_T is the characteristic turbulent time at the integral turbulent scale, $\overline{\mathbf{W}}^{(s)} = \nabla \times \overline{\mathbf{U}}^{(s)}$ is the mean vorticity characterised the semi-organised structure, the mean velocity $\overline{\mathbf{U}}^{(s)} = \overline{\mathbf{U}}_h^{(s)} + \overline{\mathbf{U}}_z^{(s)}$ that is decomposed into the horizontal $\overline{\mathbf{U}}_h^{(s)}$ and vertical $\overline{\mathbf{U}}_z^{(s)}$ components. The new contributions to the turbulent flux of potential temperature are caused by anisotropic velocity fluctuations and depend on the mean velocity gradients of the nonuniform large-scale flow. It has been demonstrated in Refs. [38, 39, 49, 71] that these new contributions cause the excitation of large-scale convective-wind instability and formation of large-scale semi-organised structures.

The mechanism of the large-scale convective-wind instability is related to the second term $\mathbf{F}_{\text{new}} = -t_T \alpha \mathbf{F}_z^* \operatorname{div} \overline{\mathbf{U}}_h^{(s)}$ in Eq. (1) for the turbulent flux of potential temperature which causes the redistribution of the vertical background turbulent flux of potential temperature \mathbf{F}_z^* by the perturbations of the convergent (or divergent) horizontal large-scale flows $\overline{\mathbf{U}}_h^{(s)}$ (see Fig. 1) during the life-time of turbulent eddies. Therefore, this effect increases the vertical turbulent flux of potential temperature by the converging horizontal motions, which enhances both, the upward (positive) turbulent flux of potential temperature and buoyancy. The latter forms the upward flow, strengthens the horizontal convergent flow resulting in the large-scale convective-wind instability.

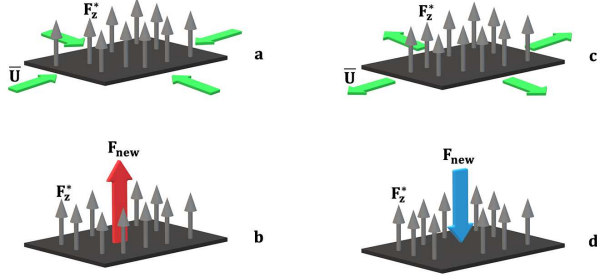


FIG. 1. The mechanism of the large-scale convective-wind instability associated with the new contribution of the turbulent flux of potential temperature $\mathbf{F}_{\text{new}} = -t_T \alpha \mathbf{F}_z^* \text{div} \bar{\mathbf{U}}_h^{(s)}$, which increases (or decreases) the vertical turbulent flux of potential temperature shown by the red arrow in **b** (or by the blue arrow in **d**) via redistribution of the uniform vertical turbulent flux \mathbf{F}_z^* by convergent (or divergent) horizontal mean flows $\bar{\mathbf{U}}_h^{(s)}$ (shown by the green arrows in **a** and **c**). The vertical turbulent flux \mathbf{F}_{new} enhances the upward (positive) turbulent flux of potential temperature, increasing the local mean potential temperature and producing the upward large-scale flow. Likewise, the vertical turbulent flux \mathbf{F}_{new} decreases the vertical turbulent flux of potential temperature by the divergent horizontal motions, decreasing the local mean potential temperature and producing the downward large-scale flow.

On the other hand, the last term $\propto (2\alpha + 3)t_T/10) (\bar{\mathbf{W}}^{(s)} \times \mathbf{F}_z^*)$ in Eq. (1) produces the horizontal turbulent flux of potential temperature by a "rotation" of the vertical background turbulent flux \mathbf{F}_z^* with the perturbations of the horizontal mean vorticity $\bar{\mathbf{W}}_h^{(s)}$. In other words, the contribution to the turbulent flux of potential temperature $\propto (2\alpha + 3)t_T/10) (\bar{\mathbf{W}}^{(s)} \times \mathbf{F}_z^*)$ creates the horizontal turbulent flux of potential temperature via rotation of the vertical turbulent flux \mathbf{F}_z^* by the large-scale horizontal vorticity, $\bar{\mathbf{W}}_h^{(s)}$, decreasing the local potential temperature in rising motions. The latter weakens the buoyancy acceleration, and reduces perturbations of the vertical large-scale velocity and vorticity, contributing to the damping of large-scale convective-wind instability [38, 39, 49].

B. Analytical solution for semi-organised structures

Let us determine the large-scale velocity $\bar{\mathbf{U}}^{(s)}$ and potential temperature $\bar{\Theta}^{(s)}$ of the semi-organised structures formed in small-scale convective turbulence. Note that the timescale of the growth of the CBL height is much larger than the characteristic time scale of evolution of the semi-organised structures [8]. During formation of these coherent structures there is a two-way nonlinear coupling:

- the effect of small-scale turbulent convection on the formed semi-organised coherent structures; and

- a back-reaction of the formed semi-organised coherent structures on small-scale turbulent convection.

The velocity and potential temperature of the semi-organised coherent structures is strongly non-uniform, that causes an anisotropy of convective turbulence. In particular, the convective plumes are extended in vertical direction in regions with strong buoyancy. To describe such complicated process, we have to solve non-linear equations for turbulence and mean-field equations for semi-organised structures simultaneously. This cannot be done analytically for large Reynolds and Rayleigh numbers. To solve this problem, we apply another approach. We use a linearized mean-field equations for the velocity and potential temperature of the semi-organised coherent structures with the parameterised turbulent flux of potential temperature determined by Eq. (1). This allows us to describe direct coupling of small-scale convective turbulence with the formed semi-organised coherent structures. However, to take into account back-reaction of the formed semi-organised coherent structures on small-scale convective turbulence, we introduce a phenomenological parameter α that determines a thermal anisotropy and describes an anisotropic form of plumes [see Eq. (20) in Sec. III C]. In such phenomenological approach we take into account the back-reaction of the coherent structures on small-scale convective turbulence.

The equations for evolution of the vorticity $\bar{\mathbf{W}}^{(s)}$ and potential temperature $\bar{\Theta}^{(s)}$ of semi-organised structures in a fluid flow in the Boussinesq approximation are given by

$$\frac{D\bar{\mathbf{W}}^{(s)}}{Dt} = K_M \Delta \bar{\mathbf{W}}^{(s)} - \beta (\mathbf{e} \times \nabla) \bar{\Theta}^{(s)} + (\bar{\mathbf{W}}^{(s)} \cdot \nabla) \bar{\mathbf{U}}^{(s)}, \quad (2)$$

$$\frac{D\bar{\Theta}^{(s)}}{Dt} = -(\nabla \cdot \mathbf{F}), \quad (3)$$

where the turbulent flux of potential temperature \mathbf{F} is given by Eq. (1). Here \mathbf{e} is the vertical unit vector, $\beta = g/T_*$ is the buoyancy parameter, \mathbf{g} is the gravity acceleration and $D/Dt = \partial/\partial t + \bar{\mathbf{U}}^{(s)} \cdot \nabla$. We restrict our consideration to the quasi-stationary regime and search for axisymmetric (ϑ -independent) solution to equations for the vorticity $\bar{\mathbf{W}}^{(s)}$ and potential temperature $\bar{\Theta}^{(s)}$, in cylindrical coordinates (r, ϑ, z) , where the velocity $\bar{\mathbf{U}}^{(s)}$ and vorticity $\bar{\mathbf{W}}^{(s)}$ are expressed in terms of the stream function Ψ as

$$\bar{\mathbf{U}}^{(s)} = -\mathbf{e}_r \frac{\partial \Psi}{\partial z} + \mathbf{e}_z \frac{1}{r} \frac{\partial(r\Psi)}{\partial r}, \quad (4)$$

$$\bar{\mathbf{W}}^{(s)} = -\mathbf{e}_\vartheta (\Delta - r^{-2}) \Psi. \quad (5)$$

Taking the eddy viscosity K_M and eddy conductivity K_H independent of r and z , linearized equations (2) and (3), we obtain the following steady-state solution:

$$\overline{U}_r^{(s)} = -A_* \overline{U}_{z0} J_1 \left(\frac{\lambda r}{R} \right) \cos \left(\frac{\pi z}{L_z} \right), \quad (6)$$

$$\overline{U}_z^{(s)} = \overline{U}_{z0} J_0 \left(\frac{\lambda r}{R} \right) \sin \left(\frac{\pi z}{L_z} \right), \quad (7)$$

$$\overline{\Theta}^{(s)} = \overline{\Theta}_0 J_0 \left(\frac{\lambda r}{R} \right) \sin \left(\frac{\pi z}{L_z} \right), \quad (8)$$

where

$$\Psi = \Psi_0 J_1 \left(\frac{\lambda r}{R} \right) \sin \left(\frac{\pi z}{L_z} \right), \quad (9)$$

$$\overline{W}^{(s)} = e_\vartheta \frac{\lambda \overline{U}_{z0}}{R} (1 + A_*^2) J_1 \left(\frac{\lambda r}{R} \right) \sin \left(\frac{\pi z}{L_z} \right), \quad (10)$$

and $J_m(x)$ is the Bessel function of the first kind possessing the properties: $2J'_m(x) = J_{m-1}(x) - J_{m+1}(x)$ and $J'_0(x) = -J_1(x)$. Here $\lambda = 3.83$ is the first root of equation $J_1(x) = 0$, so that $J_1(\lambda) = 0$, and $A_* = \pi R/(\lambda L_z)$ is aspect ratio of the semi-organised structures, where R and L_z are the radius and height of the semi-organised structures; \overline{U}_{z0} , $\overline{\Theta}_0$ and $\Psi_0 = \overline{U}_{z0} L_z$ are amplitudes of the velocity, temperature and stream-function, respectively. Substituting Eqs. (6)–(10) into Eqs. (2)–(5), we obtain relationships for the amplitudes and the aspect ratio of the semi-organised structures as

$$\frac{\overline{U}_{z0}}{\overline{\Theta}_0} = \frac{\beta L_z^2}{\pi^2 K_M} \frac{A_*^2}{(1 + A_*^2)^2}, \quad (11)$$

$$\frac{K_M^2}{\beta F_z t_T R^2 \text{Pr}_T} = \frac{\sigma (A_*^2 - \mu)}{\lambda^2 (1 + A_*^2)^2}, \quad (12)$$

$$\Psi_0 = \frac{\overline{U}_{z0} R}{\lambda}, \quad (13)$$

where $\text{Pr}_T = K_M/K_H$ is the turbulent Prandtl number, $\sigma = 4(8\alpha - 3)/45$ and $\mu = (2\alpha + 3)/(8\alpha - 3)$, and α is the degree of thermal anisotropy defined by Eq. (20) in Sec. III C. The above solution mimic comparatively narrow uprising flow surrounded by wider and weaker down-draught in reasonable agreement with large-eddy simulations [40].

III. TURBULENCE IN CBL CORE

To describe turbulence in the CBL core, we use the budget equations for the density of turbulent kinetic energy, the intensity of potential temperature fluctuations and turbulent fluxes of potential temperature and momentum in the Boussinesq approximation (see, e.g., Ref. [69]). We consider a shear-free turbulent convection with negligibly small mean velocity $\overline{U}^{(m)}$ in comparison with the velocity $\overline{U}^{(s)}$ of the semi-organised structures.

A. Budget equations

We start with the basic equations of the energy and flux budget (EFB) closure theory. The budget equation for the density of turbulent kinetic energy (TKE), $E_K = \langle \mathbf{u}^2 \rangle / 2$, the intensity of potential temperature fluctuations $E_\theta = \langle \theta^2 \rangle / 2$, the turbulent flux $F_i = \langle u_i \theta \rangle$ of potential temperature, and the Reynolds stress $\tau_{ij} = \langle u_i u_j \rangle$ are given by

$$\frac{DE_K}{Dt} + \nabla_j \Phi_j^{(K)} = -\tau_{ij} \nabla_j \overline{U}_i^{(s)} + \beta F_z - \varepsilon_K, \quad (14)$$

$$\frac{DE_\theta}{Dt} + \nabla_j \Phi_j^{(\theta)} = -(\mathbf{F} \cdot \nabla) \overline{\Theta}^{(s)} - F_z \nabla_z \overline{\Theta}^{(m)} - \varepsilon_\theta, \quad (15)$$

$$\begin{aligned} \frac{\partial F_i}{\partial t} + \nabla_j \Phi_{ij}^{(F)} &= -\tau_{iz} \nabla_z \overline{\Theta}^{(m)} - \tau_{ij} \nabla_j \overline{\Theta}^{(s)} + 2\beta E_\theta \delta_{i3} \\ &\quad - \frac{1}{\rho_0} \langle \theta \nabla_i p \rangle - (\mathbf{F} \cdot \nabla) \overline{U}_i^{(s)} - \varepsilon_i^{(F)}, \end{aligned} \quad (16)$$

$$\begin{aligned} \frac{D\tau_{ij}}{Dt} + \nabla_k \Phi_{ijk}^{(\tau)} &= -\tau_{ik} \nabla_k \overline{U}_j^{(s)} - \tau_{jk} \nabla_k \overline{U}_i^{(s)} + Q_{ij} \\ &\quad + \beta (F_i \delta_{j3} + F_j \delta_{i3}) - \varepsilon_{ij}^{(\tau)}, \end{aligned} \quad (17)$$

where $D/Dt = \partial/\partial t + \overline{U}^{(s)} \cdot \nabla$ is the convective derivative and δ_{ij} is the Kronecker unit tensor. The first term, $-\tau_{ij} \nabla_j \overline{U}_i^{(s)}$, in the RHS of Eq. (14) is the rate of production of TKE by the gradients of the velocity $\overline{U}^{(s)}$ of the semi-organised structures. In particular, turbulence in the CBL-core is produced largely by local shears in semi-organised structures. We will show that the turbulent kinetic energy is very low compared to kinetic energy of motions in semi-organised structures. These conclusions are fully confirmed by LES and various laboratory experiments (see, e.g., Ref. [40], and references therein). The second production term βF_z in Eq. (14) describes buoyancy. The first two terms, $-(\mathbf{F} \cdot \nabla) \overline{\Theta}^{(s)}$ and $-F_z \nabla_z \overline{\Theta}^{(m)}$, in the RHS of Eq. (15) are the rates of production of potential temperature fluctuations, where

the first contribution due to semi-organised structures is dominant one.

The first term, $-\tau_{iz} \nabla_z \bar{\Theta}^{(m)}$, in the RHS of Eq. (16) is the turbulent flux of potential temperature due to the small vertical gradient of the mean potential temperature, while the second term, $-\tau_{ij} \nabla_j \bar{\Theta}^{(s)}$, contributes to the turbulent flux caused by the semi-organised structures. Both terms correspond to the classical gradient mechanism of the turbulent heat transfer. The third term $2\beta E_\theta \delta_{i3}$ in the RHS of Eq. (16) describes a non-gradient contribution to the turbulent flux of potential temperature.

The term, $\varepsilon_K = \nu \langle (\nabla_j u_i)^2 \rangle$, in the RHS of Eq. (14) is the dissipation rate of the density of the turbulent kinetic energy, where ν is the kinematic viscosity of fluid. The term, $\varepsilon_\theta = \chi \langle (\nabla \theta)^2 \rangle$ in the RHS of Eq. (15) is the dissipation rate of the intensity of potential temperature fluctuations E_θ , and χ is the molecular temperature diffusivity. The term, $\varepsilon_i^{(F)} = (\nu + \chi) \langle (\nabla_j u_i) (\nabla_j \theta) \rangle$ in the RHS of Eq. (16) is the dissipation rate of the turbulent flux of potential temperature. The term, $\varepsilon_{ij}^{(\tau)} = 2\nu \langle (\nabla_k u_i) (\nabla_k u_j) \rangle$ in the RHS of Eq. (17) is the molecular-viscosity dissipation rate, and the tensor $Q_{ij} = \rho_0^{-1} (\langle p \nabla_i u_j \rangle + \langle p \nabla_j u_i \rangle)$ describes correlations of pressure fluctuations and turbulent velocity gradients.

The term $\Phi_j^{(K)} = \rho_0^{-1} \langle u_j p \rangle + (\langle u_j u^2 \rangle - \nu \nabla_j \langle u^2 \rangle) / 2$ in Eq. (14) determines the flux of E_K , where ρ_0 is the fluid density. The term $\Phi_j^{(\theta)} = (\langle u_j \theta^2 \rangle - \chi \nabla_j \langle \theta^2 \rangle) / 2$ in Eq. (15) describes the flux of E_θ . The term $\Phi_{ij}^{(F)} = \langle u_i u_j \theta \rangle - \nu \langle \theta (\nabla_j u_i) \rangle - \chi \langle u_i (\nabla_j \theta) \rangle$ in Eq. (16) determines the flux of F_i . The term $\Phi_{ijk}^{(\tau)} = \langle u_i u_j u_k \rangle + \rho_0^{-1} (\langle p u_i \rangle \delta_{jk} + \langle p u_j \rangle \delta_{ik}) - \nu [\langle u_i (\nabla_k u_j) \rangle + \langle u_j (\nabla_k u_i) \rangle]$ in Eq. (17) describes the flux of τ_{ij} . Different effects related to budget equations (14)–(17) in a stratified turbulence have been discussed in a number of publications [9, 24, 44, 45, 48, 65–69, 72, 73].

B. Basic assumptions

In the framework of the energy and flux budget turbulence closure theory, we assume the following. The characteristic times of variations of the densities of the TKE, the potential temperature fluctuations intensity, the turbulent flux of potential temperature and the Reynolds stress are substantially longer than the turbulent timescales. This assumption yields the steady-state solutions of the budget equations (14)–(17).

This allows one to express the dissipation rates of E_K , E_θ and F_i applying the Kolmogorov hypothesis. This implies that $\varepsilon_K = E_K / t_T$, $\varepsilon_\theta = E_\theta / (C_p t_T)$, and $\varepsilon_i^{(F)} = F_i / (C_F t_T)$, where $t_T = \ell_z / E_z^{1/2}$ is the turbulent dissipation timescale, ℓ_z is the vertical integral scale, and C_p and C_F are dimensionless empirical constants [1, 2, 11, 12, 15]. In addition, the dissipation rates ε_α of the TKE components $E_\alpha = \tau_{\alpha\alpha}$ with $\alpha = x, y, z$ are

$\varepsilon_x = \varepsilon_y = \varepsilon_z = E_K / 3t_T$ (see Ref. [74]), since the dominant contribution to E_α is from the Kolmogorov viscous scale where turbulence is nearly isotropic. Here the summation convention for the double Greek indices is not applied.

The term $\varepsilon_i^{(\tau)} = \varepsilon_{iz}^{(\tau)} - \beta F_i - Q_{iz}$ in Eq. (17) is the effective dissipation rate of the off-diagonal components of the Reynolds stress τ_{iz} [24, 65, 68]. The dissipation rate of τ_{iz} is assumed to be due to the combination $\varepsilon_{iz}^{(\tau)} - \beta F_i - Q_{iz}$, where $\varepsilon_{iz}^{(\tau)} = \tau_{iz} / (C_\tau t_T)$. Here C_τ is the effective-dissipation time-scale empirical constant [24, 65, 68, 69].

The effective dissipation assumption was justified by Large Eddy Simulations (see Fig. 1 in Ref. [24]), where the data from Ref. [75, 76] were used for the two types of atmospheric boundary layer: “nocturnal stable” (with essentially negative buoyancy flux at the surface and neutral stratification in the free flow) and “conventionally neutral” (with a negligible buoyancy flux at the surface and essentially stably stratified turbulence in the free flow). The effective dissipation assumption directly yields the well-known down-gradient formulation of the vertical turbulent flux of momentum

$$\langle u_i u_z \rangle = -K_M \nabla_z \bar{U}_i, \quad (18)$$

where $i = x, y$, and

$$K_M = 2C_\tau t_T E_z = 2C_\tau \ell_z E_z^{1/2}. \quad (19)$$

The latter result is valid for a shear-produced turbulence or a convective turbulence with a non-uniform large-scale velocity field. We point out that the diagonal components of the Reynolds stress are much larger than the off-diagonal components. The diagonal components of the Reynolds stress determines the TKE components which obey the Kolmogorov spectrum $\propto k^{-5/3}$, while the off-diagonal components of the Reynolds stress are produced by the tangling mechanism of generation of anisotropic velocity fluctuations, and they obey the $\propto k^{-7/3}$ spectrum [77–80].

The final assumption is related to the term $\rho_0^{-1} \langle \theta \nabla_z p \rangle$ in the budget equation for F_z which is parameterised as $\beta \langle \theta^2 \rangle - \rho_0^{-1} \langle \theta \nabla_z p \rangle = 2C_\theta \beta E_\theta$, where $C_\theta < 1$ is the positive dimensionless empirical constant. The latter assumption has been justified analytically (see Appendix A in [65]) and by Large Eddy Simulations, where the data from Refs. [75, 76] have been used for the two types of atmospheric boundary layer: “nocturnal stable” and “conventionally neutral” (see Fig. 2 in [24]).

For convective turbulence, we choose the following values of the non-dimensional empirical constants which have been used in the EFB theory for stably stratified turbulence [68, 69]: $C_p = 0.417$, $C_\theta = 0.744$, $C_\tau = 0.1$ and $C_F = 0.125$. This corresponds to the turbulent Prandtl number for a non-stratified turbulence $\text{Pr}_T^{(0)} = 0.8$.

C. Global characteristics of convective turbulence with semi-organised structures

In this section we determine global characteristics of convective turbulence by averaging over the entire volume of the semi-organised structure. As follows from laboratory experiments [81, 82], direct numerical simulations [83–86], and mean-field numerical simulations [71], the vertical gradient of the mean potential temperature can be positive and negative inside the large-scale circulations in a convective turbulence. In particular, the vertical gradient of the mean potential temperature can be positive when the vertical turbulent flux of potential temperature is negative.

To describe this effect, we introduce the degree of thermal anisotropy α in convective turbulence that depends on the form of plumes. In particular, the plumes can be characterised by the two-point instantaneous correlation function $\langle \theta(t, \mathbf{x}) u_z(t, \mathbf{x} + \mathbf{r}) \rangle$, where $\ell_h^{(pl)}$ and $\ell_z^{(pl)}$ are the horizontal and vertical scales in which the two-point instantaneous correlation functions $\langle \theta(t, \mathbf{x}) u_z(t, \mathbf{x} + \mathbf{r}) \rangle$ tend to 0 in the horizontal and vertical directions, respectively. The degree of thermal anisotropy α is defined as [38]

$$\alpha = -3 \left(\frac{3 - 4 \left(\ell_h^{(pl)} / \ell_z^{(pl)} \right)^{\frac{2}{3}}}{2 + \left(\ell_h^{(pl)} / \ell_z^{(pl)} \right)^{\frac{2}{3}}} \right). \quad (20)$$

For isotropic case $\ell_h^{(pl)} = \ell_z^{(pl)}$ when the plumes have the form of ball and the degree of thermal anisotropy $\alpha = 1$. For $\alpha < 1$, the plumes are extended in the vertical direction having the form of columns, $\ell_h^{(pl)} < \ell_z^{(pl)}$. For $\ell_h^{(pl)} \ll \ell_z^{(pl)}$, the parameter α can be estimated as

$$\alpha \approx -\frac{9}{2} \left(1 - \frac{3}{2} \left(\frac{\ell_h^{(pl)}}{\ell_z^{(pl)}} \right)^{\frac{2}{3}} \right). \quad (21)$$

For $\alpha > 1$, the plumes have the form of “pancake”, $\ell_h^{(pl)} > \ell_z^{(pl)}$. For $\ell_h^{(pl)} \gg \ell_z^{(pl)}$, the parameter α can be estimated as

$$\alpha \approx 12 \left(1 - \frac{11}{4} \left(\frac{\ell_z^{(pl)}}{\ell_h^{(pl)}} \right)^{\frac{2}{3}} \right). \quad (22)$$

Using Eqs. (12) and (19), we determine the normalized vertical turbulent flux of potential temperature averaged over the entire volume of the semi-organised structure as

$$\langle \hat{F} \rangle_v \equiv \frac{\beta \langle F_z \rangle_v \ell}{\langle E_K^{3/2} \rangle_v} = C_\tau^2 \left(\frac{\ell_z}{L_z} \right)^2 \frac{f_{\hat{F}}(A_*)}{\text{Pr}_T}, \quad (23)$$

where $\langle \dots \rangle_v$ denote averaging over the entire volume of the semi-organised structure, $\hat{F} = \beta F_z \ell / E_K^{3/2}$, function

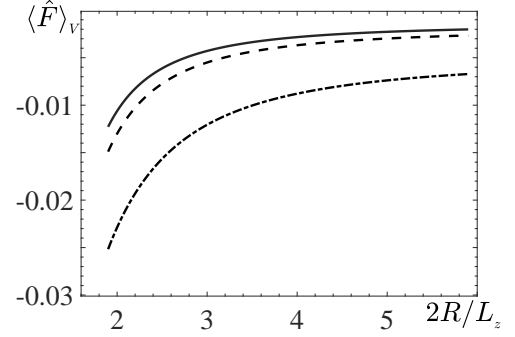


FIG. 2. The normalized vertical turbulent flux of the potential temperature $\langle \hat{F} \rangle_v$ versus the aspect ratio $2R/L_z$ of the semi-organized structures with the scale separation parameter $L_z/\ell_z = 7$ and for different values of the degree of thermal anisotropy: $\alpha = -4$, i.e., for $\ell_h^{(pl)}/\ell_z^{(pl)} = 0.1$ (solid line); $\alpha = -2.1$, i.e., for $\ell_h^{(pl)}/\ell_z^{(pl)} = 0.2$ (dashed line) and $\alpha = -0.55$, i.e., for $\ell_h^{(pl)}/\ell_z^{(pl)} = 0.5$ (dashed-dotted line).

$f_{\hat{F}}(A_*)$ is given by Eq. (A1) in Appendix A. We remind that the aspect ratio of the semi-organised structures is $A_* = \pi R/(\lambda L_z)$ (see Sec. II). Here we assume that the turbulent dissipation timescale is $t_T = \ell_z/E_z^{1/2} = \ell/E_K^{1/2}$ and the vertical anisotropy parameter is $A_z = E_z/E_K = (\ell_z/\ell)^2 = 1/3$. It follows from Eq. (23) that $\langle \hat{F} \rangle_v \ll 1$ since $\ell_z \ll L_z$ and coefficient C_τ is small. This implies that the volume averaged TKE dissipation rate $\langle \varepsilon_K \rangle_v \equiv \langle E_K \rangle_v / t_T = \langle E_K^{3/2} \rangle_v / \ell$, is much larger than turbulence production, $\beta \langle F_z \rangle_v$, caused by buoyancy. This is due to the fact that for large Rayleigh numbers, the convective turbulence is mainly produced by the local shear of the semi-organized structures rather than the buoyancy (see below).

As follows from Eqs. (23) and Eq. (A1) in Appendix A, the vertical flux of potential temperature $\langle F_z \rangle_v$ is negative when $f_{\hat{F}}(A_*) < 0$, i.e.,

$$2\alpha (4A_*^2 - 1) < 3(1 + A_*^2). \quad (24)$$

This implies that the vertical flux of potential temperature $\langle F_z \rangle_v$ is negative when

$$-\frac{9}{2} < \alpha < \frac{3(1 + A_*^2)}{2(4A_*^2 - 1)}, \quad (25)$$

where we use Eqs. (21) and (24). Note that the large-scale circulations are formed when $A_* \geq 1$ [38, 39]. Applying Eqs. (20) and (25), we obtain that the vertical flux of potential temperature $\langle F_z \rangle_v$ is negative when

$$\left(\frac{\ell_h^{(pl)}}{\ell_z^{(pl)}} \right)^{\frac{2}{3}} < \frac{2(13A_*^2 - 2)}{31A_*^2 - 9}. \quad (26)$$

In Fig. 2 we plot the normalized vertical turbulent flux of the potential temperature $\langle \hat{F} \rangle_v \equiv \beta \langle F_z \rangle_v \ell / \langle E_K^{3/2} \rangle_v$ versus the aspect ratio $2R/L_z$ of the semi-organized

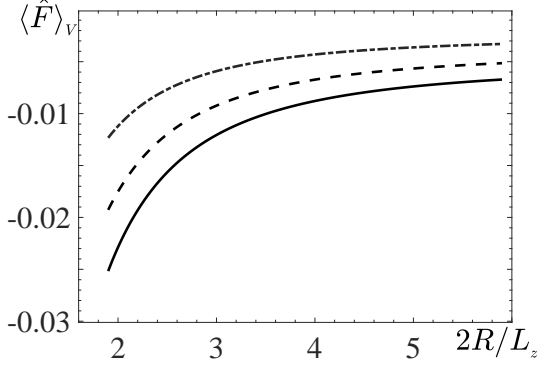


FIG. 3. The normalized vertical turbulent flux of the potential temperature $\langle \hat{F} \rangle_V \equiv \beta \langle F_z \rangle_V \ell / \langle E_K^{3/2} \rangle_V$ versus the aspect ratio $2R/L_z$ of the semi-organized structures for $\alpha = -0.55$ and different values of the scale separation parameter $L_z/\ell_z = 7$ (solid line); 8 (dashed line) and 10 (dashed-dotted line).

structures for different values of the degree of thermal anisotropy α . Here we take into account that semi-organized structures are formed when the scale separation parameter is $L_z/\ell_z > 5$ and the aspect ratio for the semi-organized structures is $2R/L_z \geq 2$ [38, 39]. It is seen in Fig. 2 that when plumes are extended in the vertical direction, i.e., $\ell_h^{(pl)}/\ell_z^{(pl)} < 1$, the vertical turbulent flux of potential temperature $\langle F_z \rangle_V$ is negative.

In Fig. 3 we also show the dependence of the normalized vertical turbulent flux of the potential temperature $\langle \hat{F} \rangle_V$ on the aspect ratio $2R/L_z$ of the semi-organized structures for $\alpha = -0.55$ ($\ell_h^{(pl)}/\ell_z^{(pl)} = 0.5$) and different values of the scale separation parameter L_z/ℓ_z . The absolute value of the normalized vertical turbulent flux of potential temperature decreases with increase of scale separation between vertical size of the semi-organized structures L_z and the vertical integral scale ℓ_z .

The production rate, Π_K , of the turbulent kinetic energy by local large-scale shear $\nabla_j \bar{U}_i^{(s)}$ of the semi-organized structures is given by $\Pi_K = -\tau_{ij} \nabla_j \bar{U}_i^{(s)} = 2K_M S^2$ [see the first term in the RHS of Eq. (14)], where S is the large-scale shear. Using the steady-state version of the budget equation (14), we obtain that turbulent kinetic energy is $E_K = 4C_\tau \ell_z^2 S^2 / (1 - \hat{F})$. To determine the volume averaged production rate of the turbulent kinetic energy, we use the analytical solution (6)–(7) for the velocity $\bar{U}^{(s)}$ of the semi-organized structure. In particular, the squared large-scale shear $\langle S^2 \rangle_V$ averaged over the entire volume of the semi-organized structure is given by

$$\begin{aligned} \langle S^2 \rangle_V &= \left\langle \left(\nabla_r \bar{U}_r^{(s)} \right)^2 \right\rangle_V + \left\langle \left(\nabla_z \bar{U}_z^{(s)} \right)^2 \right\rangle_V \\ &+ \frac{1}{2} \left\langle \left(\nabla_r \bar{U}_z^{(s)} + \nabla_z \bar{U}_r^{(s)} \right)^2 \right\rangle_V = \frac{1}{4} \left(\frac{\bar{U}_{z0}}{R} \right)^2 \tilde{f}_S(A_*), \end{aligned} \quad (27)$$

where the function $\tilde{f}_S(A_*)$ is given by Eq. (A2) in Appendix A. To derive Eq. (27), we use Eqs. (B1)–(B4) in Appendix B. Therefore, the volume averaged turbulent kinetic energy density is given by

$$\langle E_K \rangle_V = C_\tau \left(\frac{\ell_z}{L_z} \right)^2 \bar{U}_{z0}^2 \frac{f_S(A_*)}{1 - \langle \hat{F} \rangle_V}, \quad (28)$$

where the function $f_S(A_*)$ is given by Eq. (A3) in Appendix A. Equation (28) implies that the turbulent kinetic energy density $\langle E_K \rangle_V$ is much less than the squared velocity \bar{U}_{z0}^2 .

The vertical flux of potential temperature, $\langle \bar{\Theta}^{(s)} \bar{U}_z^{(s)} \rangle_V$, transported by the semi-organized structures, is determined using Eqs. (11) and (28), and Eq. (B5) in Appendix B:

$$\langle \bar{\Theta}^{(s)} \bar{U}_z^{(s)} \rangle_V = C_\tau^{3/2} \left(\frac{\ell_z^2 \bar{U}_{z0}^3}{L_z^3 \beta} \right) \frac{f_{F_s}(A_*)}{(1 - \langle \hat{F} \rangle_V)^{1/2}} \quad (29)$$

where function $f_{F_s}(A_*)$ is given by Eq. (A4) in Appendix A. By means of Eq. (29), we find a characteristic convective velocity U_D defined as

$$\begin{aligned} U_D &\equiv \left(\beta \langle \bar{\Theta}^{(s)} \bar{U}_z^{(s)} \rangle_V L_z \right)^{1/3} \\ &= \bar{U}_{z0} C_\tau^{1/2} \left(\frac{\ell_z}{L_z} \right)^{2/3} \frac{f_{F_s}^{1/3}(A_*)}{(1 - \langle \hat{F} \rangle_V)^{1/6}}. \end{aligned} \quad (30)$$

Now we define a characteristic convective temperature Θ_D from a condition

$$\Theta_D U_D = \langle \bar{\Theta}^{(s)} \bar{U}_z^{(s)} \rangle_V. \quad (31)$$

Using the definition (30) of the convective velocity U_D , we obtain a relation between the convective velocity U_D and the convective temperature Θ_D as $U_D = (\beta L_z \Theta_D)^{1/2}$. By means of Eq. (30) and Eq. (B5) in Appendix B, we find the convective temperature Θ_D as

$$\Theta_D = \bar{\Theta}_0 \left(\frac{\ell_z}{L_z} \right)^{-2/3} \frac{(1 - \langle \hat{F} \rangle_V)^{1/6}}{2C_\tau^{1/2} f_{F_s}^{1/3}(A_*)} J_0^2(\lambda). \quad (32)$$

The velocity U_D and temperature Θ_D characterise the large-scale properties of convection.

Let us determine the global energetic characteristics of semi-organized structures. Equations (30) and (B6) in Appendix B yield an expression for the kinetic energy density of semi-organized structures as

$$\begin{aligned} \langle E_U \rangle_V &\equiv \frac{1}{2} \left[\left\langle \left(\bar{U}_z^{(s)} \right)^2 \right\rangle_V + \left\langle \left(\bar{U}_r^{(s)} \right)^2 \right\rangle_V \right] \\ &= \frac{U_D^2}{C_\tau} \left(\frac{L_z}{\ell_z} \right)^{4/3} (1 - \langle \hat{F} \rangle_V)^{1/3} f_U(A_*), \end{aligned} \quad (33)$$

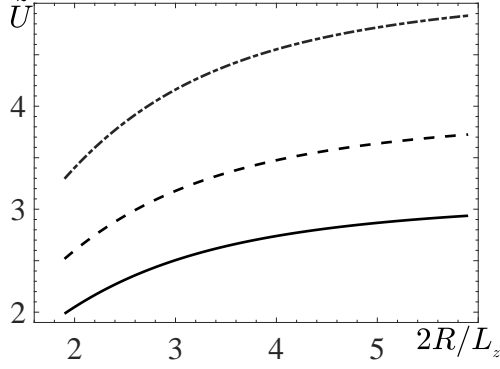


FIG. 4. The normalized velocity $\tilde{U} = \sqrt{2\langle E_U \rangle_v} / U_D$ versus the aspect ratio $2R/L_z$ of the semi-organized structures for $\alpha = -0.55$ and different values of the scale separation parameter $L_z/\ell_z = 7$ (solid line); 8 (dashed line) and 10 (dashed-dotted line).

where function $f_U(A_*)$ is given by Eq. (A5) in Appendix A. In Fig. 4 we show the normalized velocity $\tilde{U} = \sqrt{2\langle E_U \rangle_v} / U_D$ versus the aspect ratio $2R/L_z$ of the semi-organized structures for different values of the scale separation parameter L_z/ℓ_z . The kinetic energy density $\langle E_U \rangle_v$ of the semi-organised structures increases with increase of the scale separation parameter L_z/ℓ_z [see Eq. (33)]. Note that the kinetic energy density $\langle E_U \rangle_v$ is nearly independent of the parameter α (and the ratio $\ell_h^{(pl)}/\ell_z^{(pl)}$) which characterises the thermal anisotropy of convective turbulence.

Equation (32) and Eq. (B7) in Appendix B yield the thermal energy of the semi-organised structures as

$$\begin{aligned} \langle E_\Theta \rangle_v &\equiv \frac{1}{2} \left\langle \left(\overline{\Theta}^{(s)} \right)^2 \right\rangle_v \\ &= \Theta_D^2 C_\tau \left(\frac{\ell_z}{L_z} \right)^{\frac{4}{3}} \frac{f_\Theta(A_*)}{(1 - \langle \hat{F} \rangle_v)^{1/3}}, \end{aligned} \quad (34)$$

where function $f_\Theta(A_*)$ is given by Eq. (A6) in Appendix A. In Fig. 5 we plot the normalized temperature $\tilde{\Theta} = \sqrt{2\langle E_\Theta \rangle_v} / \Theta_D$ versus the aspect ratio $2R/L_z$ of the semi-organized structures for different values of the scale separation parameter L_z/ℓ_z . Equation (34) and Fig. 5 demonstrate that the thermal energy of the semi-organised structure $\langle E_\Theta \rangle_v$ increases with the aspect ratio $2R/L_z$ of the semi-organized structures approaching to the value which is of the order of Θ_D^2 .

Using Eqs. (28) and (30), we express the turbulent kinetic energy density $\langle E_K \rangle_v$ in terms of the squared convective velocity U_D^2 as

$$\langle E_K \rangle_v = U_D^2 \left(\frac{\ell_z}{L_z} \right)^{\frac{2}{3}} \frac{f_u(A_*)}{(1 - \langle \hat{F} \rangle_v)^{2/3}}, \quad (35)$$

where function $f_u(A_*)$ is given by Eq. (A7) in Appendix A. Equation (35) implies that the turbulent ki-

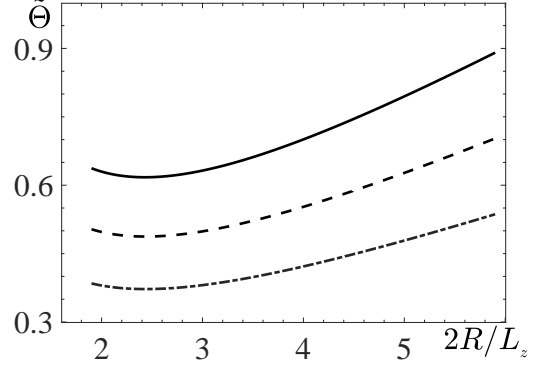


FIG. 5. The normalized temperature $\tilde{\Theta} = \sqrt{2\langle E_\Theta \rangle_v} / \Theta_D$ versus the aspect ratio $2R/L_z$ of the semi-organized structures for $\alpha = -0.55$ and different values of the scale separation parameter $L_z/\ell_z = 7$ (solid line); 8 (dashed line) and 10 (dashed-dotted line).

netic energy density is much smaller than the squared velocity U_D^2 . Equations (33) and (35) allow to determine the ratio of the turbulent kinetic energy density $\langle E_K \rangle_v$ to the kinetic energy density of semi-organised structures $\langle E_U \rangle_v$ as

$$\frac{\langle E_K \rangle_v}{\langle E_U \rangle_v} = C_\tau \left(\frac{\ell_z}{L_z} \right)^2 (1 - \langle \hat{F} \rangle_v)^{-1} \frac{f_u(A_*)}{f_U(A_*)}. \quad (36)$$

In Fig. 6 we plot the ratio of the turbulent kinetic energy density to the kinetic energy density of semi-organised structures, $\langle E_K \rangle_v / \langle E_U \rangle_v$ versus the aspect ratio $2R/L_z$ of the semi-organized structures for different values of the scale separation parameter L_z/ℓ_z . As follows from Eq. (36) and Fig. 6, the turbulent kinetic energy density $\langle E_K \rangle_v$ is much smaller than the kinetic energy density of semi-organised structures $\langle E_U \rangle_v$. Equation (35) allows us to determine the turbulent time $t_T = \ell / \sqrt{\langle E_K \rangle_v}$,

$$t_T = \sqrt{3} \frac{L_z}{U_D} \left(\frac{\ell_z}{L_z} \right)^{\frac{2}{3}} \frac{(1 - \langle \hat{F} \rangle_v)^{1/3}}{f_u^{1/2}(A_*)}, \quad (37)$$

which is much smaller than the characteristic convective time L_z/U_D for large scale separation parameter L_z/ℓ_z .

Equations (23), (28) and (29) allow us to determine the ratio of the vertical turbulent flux of potential temperature $\langle F_z \rangle_v$ to the vertical flux of potential temperature $\langle \overline{\Theta}^{(s)} \overline{U}^{(s)} \rangle_v = \Theta_D U_D$ transported by the semi-organised structures as

$$\frac{\langle F_z \rangle_v}{\Theta_D U_D} = \frac{C_\tau^2}{\text{Pr}_T} \left(\frac{\ell_z}{L_z} \right)^2 (1 - \langle \hat{F} \rangle_v)^{-1} f_{F_T}(A_*), \quad (38)$$

where function $f_{F_T}(A_*)$ is given by Eq. (A8) in Appendix A. In Fig. 7 we show the normalized vertical turbulent flux of the potential temperature $\langle F_z \rangle_v / (\Theta_D U_D)$ versus the aspect ratio $2R/L_z$ of the semi-organized

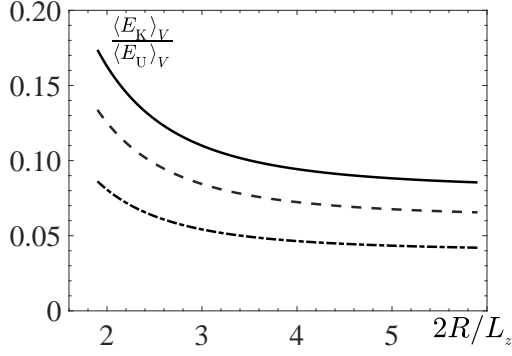


FIG. 6. The ratio of the turbulent kinetic energy density to the kinetic energy density of semi-organized structures, $\langle E_K \rangle_V / \langle E_U \rangle_V$ versus the aspect ratio $2R/L_z$ of the semi-organized structures for $\alpha = -0.55$ and different values of the scale separation parameter $L_z/\ell_z = 7$ (solid line); 8 (dashed line) and 10 (dashed-dotted line).

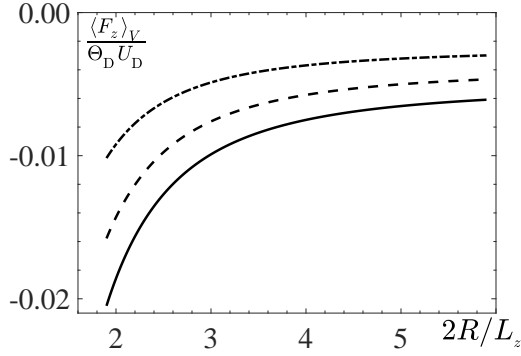


FIG. 7. The normalized vertical turbulent flux of the potential temperature $\langle F_z \rangle_V / (\Theta_D U_D)$ versus the aspect ratio $2R/L_z$ of the semi-organized structures for $\alpha = -0.55$ (i.e., for $\ell_h^{(pl)}/\ell_z^{(pl)} = 0.5$) and different values of the scale separation parameter $L_z/\ell_z = 7$ (solid line); 8 (dashed line) and 10 (dashed-dotted line).

structures for $\alpha = -0.55$ (i.e., for $\ell_h^{(pl)}/\ell_z^{(pl)} = 0.5$) and different values of the scale separation parameter L_z/ℓ_z . It follows from Eq. (38) and Fig. 7 that the vertical flux of potential temperature, $\langle \overline{\Theta}^{(s)} \overline{U}_z^{(s)} \rangle_V$, transported by the semi-organized structures is much larger than the vertical turbulent flux, $\langle F_z \rangle_V$, of potential temperature, i.e., $|\langle F_z \rangle_V| / (\Theta_D U_D) \ll 1$. Note that the analysis of large-scale instability in shear-free convection [38, 39] shows that the semi-organized structures are formed when the scale separation parameter $L_z/\ell_z > 5$.

Using Eqs. (B8)–(B12) in Appendix B, we obtain expression for the turbulent thermal energy $\langle E_\theta \rangle_V$ as

$$\langle E_\theta \rangle_V = \Theta_D^2 C_F C_p C_\tau \left(\frac{\ell_z}{L_z} \right)^{\frac{10}{3}} \frac{f_\theta(A_*)}{(1 - \langle \hat{F} \rangle_V)^{1/3}} \quad (39)$$

where function $f_\theta(A_*)$ is given by Eq. (A9) in Ap-

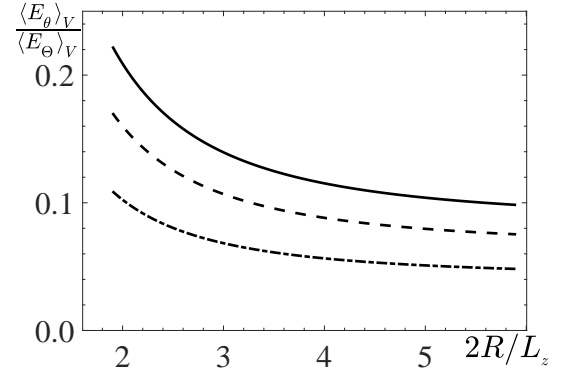


FIG. 8. The ratio of the turbulent thermal energy to the thermal energy of the semi-organized structures, $\langle E_\theta \rangle_V / \langle E_\Theta \rangle_V$, versus the aspect ratio $2R/L_z$ of the semi-organized structures for $\alpha = -0.55$ and different values of the scale separation parameter $L_z/\ell_z = 7$ (solid line); 8 (dashed line) and 10 (dashed-dotted line).

pendix A. Thus, the ratio of the turbulent thermal energy $\langle E_\theta \rangle_V$ to the thermal energy of the semi-organized structures $\langle E_\Theta \rangle_V$ is given by

$$\frac{\langle E_\theta \rangle_V}{\langle E_\Theta \rangle_V} = C_F C_p \left(\frac{\ell_z}{L_z} \right)^2 \frac{f_\theta(A_*)}{f_\Theta(A_*)}, \quad (40)$$

where we use Eq. (34). In Fig. 8 we show the ratio of the turbulent thermal energy to the thermal energy of the semi-organized structures, $\langle E_\theta \rangle_V / \langle E_\Theta \rangle_V$, versus the aspect ratio $2R/L_z$ of the semi-organized structures for different values of the scale separation parameter L_z/ℓ_z . Equation (40) and Fig. 8 demonstrate that the turbulent thermal energy $\langle E_\theta \rangle_V$ is much smaller than the thermal energy of the semi-organized structures $\langle E_\Theta \rangle_V$.

Averaging equation for the vertical turbulent flux of potential temperature [see Eq. (B8) in Appendix B] over the organised-structure volume, we obtain that

$$\langle F_z \rangle_V = -\langle K_H \rangle_V \nabla_z \overline{\Theta}^{(m)} + \langle F_z^{(W)} \rangle_V + \langle F_z^{(D)} \rangle_V. \quad (41)$$

The first term in the RHS of Eq. (41) is the classical gradient transport term that describes the eddy heat diffusivity with the turbulent diffusion coefficient $\langle K_H \rangle_V = 2C_F \ell \sqrt{\langle E_K \rangle_V}$ that is given by

$$\langle K_H \rangle_V = 2\sqrt{3}C_F L_z U_D \left(\frac{\ell_z}{L_z} \right)^{\frac{4}{3}} \frac{f_u^{1/2}(A_*)}{(1 - \langle \hat{F} \rangle_V)^{1/3}}, \quad (42)$$

where we use Eq. (35). The second term in the RHS of Eq. (41) determines a secondary vertical turbulent flux, $\langle F_z^{(W)} \rangle_V = -C_F t_T \langle F_r \nabla_r \overline{U}_z^{(s)} \rangle_V$, caused by an interaction of the horizontal turbulent flux F_r of the potential

temperature with the local shear $\nabla_r \bar{U}_z^{(s)}$ of the semi-organized structures, where the horizontal turbulent flux F_r of the potential temperature is given by Eq. (B9) in Appendix B. Using Eqs. (38) and Eq. (B13) in Appendix B, we obtain the ratio $\langle F_z^{(W)} \rangle_v / \langle F_z \rangle_v$ as

$$\frac{\langle F_z^{(W)} \rangle_v}{\langle F_z \rangle_v} = \frac{\pi^2}{\text{Pr}_T} \frac{1 - \langle \hat{F} \rangle_v}{A_*^2 f_{F_T}(A_*)}. \quad (43)$$

The last term in the RHS of Eq. (41) describes the Deardorf turbulent flux, $\langle F_z^{(D)} \rangle_v = 2C_F C_\theta t_T \beta \langle E_\theta \rangle_v$, caused by potential temperature fluctuations. Using Eqs. (35) and (38), we determine the ratio $\langle F_z^{(D)} \rangle_v / \langle F_z \rangle_v$ as

$$\frac{\langle F_z^{(D)} \rangle_v}{\langle F_z \rangle_v} = C_p C_\theta C_F \left(\frac{\ell_z}{L_z} \right)^2 \left(1 - \langle \hat{F} \rangle_v \right) f_D(A_*), \quad (44)$$

where function $f_D(A_*)$ is given by Eq. (A10) in Appendix A.

It follows from Eqs. (43) and (44) that $|\langle F_z^{(W)} \rangle_v| / |\langle F_z \rangle_v| \ll 1$ and $|\langle F_z^{(D)} \rangle_v| / |\langle F_z \rangle_v| \ll 1$. Using Eqs. (38) and (42), we obtain the final expression for the vertical gradient of the mean potential temperature, $\nabla_z \bar{\Theta}^{(m)} \approx -\langle F_z \rangle_v / \langle K_H \rangle_v$, as

$$\nabla_z \bar{\Theta}^{(m)} = -\frac{\Theta_D}{L_z} \left(\frac{\ell_z}{L_z} \right)^{\frac{2}{3}} \left(1 - \langle \hat{F} \rangle_v \right)^{-4/3} f_\nabla(A_*), \quad (45)$$

where function $f_\nabla(A_*)$ is given by Eq. (A11) in Appendix A. In Fig. 9 we plot the normalised vertical gradient of the mean potential temperature, $\nabla_z \tilde{\Theta} = (L_z / \Theta_D) \nabla_z \bar{\Theta}^{(m)}$, versus the aspect ratio $2R/L_z$ of the semi-organized structures for different values of the scale separation parameter L_z/ℓ_z . As follows from Eq. (45) and Fig. 9 that the normalised vertical gradient of the mean potential temperature $\nabla_z \tilde{\Theta}$ is small and positive, because for the considered parameter range [see Eq. (25)] the vertical turbulent flux of the potential temperature $\langle F_z \rangle_v$ is negative as well as the function $f_\nabla(A_*)$ is negative.

IV. TRANSITION FROM CBL CORE TO CONVECTIVE SURFACE LAYER

In this Section we discuss a matching of solutions obtained for the CBL core and the convective surface layer. We start with the solutions obtained for the convective surface layer.

A. Convective surface layer

First, we outline the results of the EFB theory for the atmospheric convective surface layer [69]. The verti-

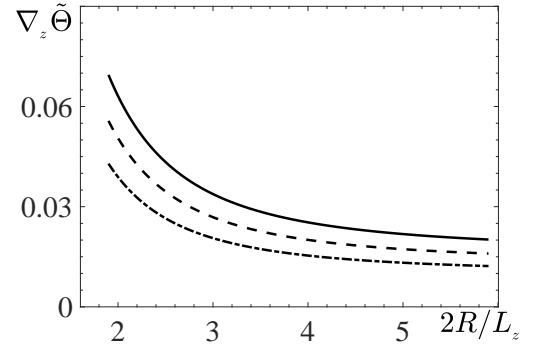


FIG. 9. The normalised vertical gradient of the mean potential temperature, $\nabla_z \tilde{\Theta} = (L_z / \Theta_D) \nabla_z \bar{\Theta}^{(m)}$, versus the aspect ratio $2R/L_z$ of the semi-organized structures for $\alpha = -0.55$ and different values of the scale separation parameter $L_z/\ell_z = 7$ (solid line); 8 (dashed line) and 10 (dashed-dotted line).

cal profiles of various turbulent characteristics are determined by the following equations:

- the flux Richardson number,

$$\text{Ri}_f(\tilde{Z}) = \tilde{Z} \left[\tilde{E}_K(\tilde{Z}) \right]^{1/2}, \quad (46)$$

- the turbulent viscosity,

$$K_M(\tilde{Z}) = u_* L_O \text{Ri}_f(\tilde{Z}), \quad (47)$$

- the turbulent Prandtl number,

$$\text{Pr}_T(\tilde{Z}) = \text{Pr}_T^{(0)} \left[1 - \frac{C_\theta C_p \text{Ri}_f(\tilde{Z})}{A_z (1 - \text{Ri}_f(\tilde{Z}))} \right]^{-1}, \quad (48)$$

- the level of temperature fluctuations,

$$E_\theta(\tilde{Z}) = \theta_*^2 C_p (2C_\tau A_z)^{-1/2} \frac{\text{Pr}_T(\tilde{Z})}{\tilde{E}_K(\tilde{Z})}, \quad (49)$$

- the large-scale shear,

$$\tilde{S}(\tilde{Z}) = \frac{u_*}{L_O \text{Ri}_f(\tilde{Z})}, \quad (50)$$

- the vertical gradient of the mean potential temperature,

$$\nabla_z \bar{\Theta}^{(m)} = \frac{\theta_* \text{Pr}_T(\tilde{Z})}{|L_O| \text{Ri}_f(\tilde{Z})}, \quad (51)$$

where $\text{Ri}_f = -\beta \tilde{F}_z / (K_M \tilde{S}^2)$ is the flux Richardson number, \tilde{F}_z is the vertical turbulent flux of the potential temperature at the surface layer, $u_*^2 = K_M \tilde{S}$ with u_* being

the local (z -dependent) friction velocity, $\tilde{S} = d\bar{U}_h^{(m)}/dz$ is the large-scale shear, $\bar{U}_h^{(m)}(z)$ is the mean horizontal velocity at the surface layer, $\theta_* = |\tilde{F}_z|/u_* = u_*^2/\beta|L_O|$ with L_O being the local Obukhov length defined as $L_O = -u_*^3/(\beta\tilde{F}_z)$, the normalised height $\tilde{Z} = \kappa_0 z/L_O$ with $\kappa_0 = 0.4$ being the von Karman constant, and $\text{Pr}_T^{(0)} = C_\tau/C_F$ is the turbulent Prandtl number for a non-stratified turbulence at $\text{Ri}_f = 0$. Note that the flux Richardson number Ri_f is negative in the convective turbulence in surface layer, and its absolute value is not limited and can be large. The local Obukhov length L_O is negative in the convective turbulence as well, but the product $L_O \text{Ri}_f$ is positive. The vertical profile of the normalised turbulent kinetic energy density, $\tilde{E}_K(\tilde{Z}) = E_K(\tilde{Z})/E_{K0}$, is determined by the following nonlinear equation:

$$\tilde{E}_K^2 + \tilde{Z} \tilde{E}_K^{1/2} - 1 = 0. \quad (52)$$

where $E_{K0} = u_*^2/(2C_\tau A_z)^{1/2}$. Asymptotic formulas for the surface layer in convective turbulence are given in Ref. [69]. Using Eq. (50), we obtain the mean horizontal velocity at the surface layer as

$$\bar{U}_h^{(m)}(z) = \frac{u_*}{\kappa_0} \int_0^z \frac{d\tilde{Z}}{\tilde{Z} [\tilde{E}_K(\tilde{Z})]^{1/2}}. \quad (53)$$

B. Matching of solutions for CBL core and convective surface layer

The matching between the solutions obtained for the CBL core and the convective surface layer are performed as follows.

- The mean potential temperature $\bar{\Theta}^{(m)}$ and the mean horizontal velocity $\bar{U}_h^{(m)}$ for the convective surface layer at $|\tilde{Z}| \gg 1$ are matched with the mean potential temperature $\bar{\Theta}^{(s)}$ and the mean velocity $\bar{U}_r^{(s)}$ for the CBL core at $\pi z/L_z \ll 1$.
- The vertical turbulent flux of potential temperature \tilde{F}_z for the convective surface layer at $|\tilde{Z}| \gg 1$ are matched with the vertical flux of potential temperature, $\langle \bar{\Theta}^{(s)} \bar{U}_z^{(s)} \rangle_v + \langle F_z \rangle_v$, transported by both, the semi-organised structures and turbulence at $\pi z/L_z \ll 1$.

As the result, the ratio of the local Obukhov length scale, $L_O = -u_*^3/(\beta\tilde{F}_z)$, for the convective surface layer to the vertical size of the semi-organised structure L_z is $L_O/L_z = -(u_*/U_D)^3$, where the convective velocity U_D in this case is $U_D = (\beta\tilde{F}_z L_z)^{1/3}$, and we take into account that $\left| \langle \bar{\Theta}^{(s)} \bar{U}_z^{(s)} \rangle_v \right| \gg |\langle F_z \rangle_v|$. Using Eqs. (6),

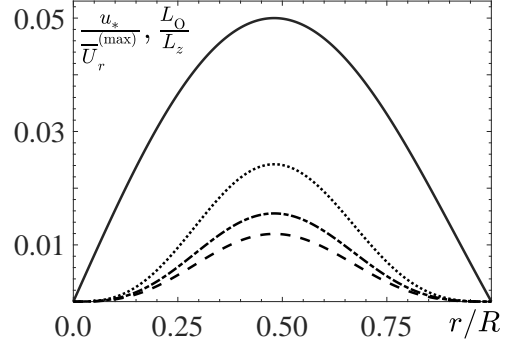


FIG. 10. The radial profiles of the ratio L_O/L_z for different values of the scale separation parameter $L_z/\ell_z = 7$ (dashed line); 8 (dashed-dotted line) and 10 (dotted line); the radial profile of the ratio $u_*/\bar{U}_r^{(\max)}$ (solid line).

(30) and (53), we obtain the ratio of the friction velocity u_* to the convective velocity U_D as

$$\frac{u_*}{U_D} = \frac{\kappa_0 A_* \left(1 - \langle \hat{F} \rangle_v\right)^{1/6}}{C_\tau^{1/2} f_{F_s}^{1/3}(A_*) I_U} \left(\frac{L_z}{\ell_z}\right)^{2/3} J_1\left(\frac{\lambda r}{R}\right), \quad (54)$$

where $\bar{U}_h^{(m)}(|\tilde{Z}| \gg 1) \approx u_* I_U/\kappa_0$ and

$$I_U = \int_0^\infty \frac{d\tilde{Z}}{\tilde{Z} [\tilde{E}_K(\tilde{Z})]^{1/2}}. \quad (55)$$

The ratio of the friction velocity u_* to the maximum value $\bar{U}_r^{(\max)}$ of the horizontal velocity of the semi-organized structure $\bar{U}_r^{(s)}$ is given by

$$\frac{u_*}{\bar{U}_r^{(\max)}} = \frac{\kappa_0}{I_U} \frac{J_1(\lambda r/R)}{J_1(\lambda r_{\max}/R)}, \quad (56)$$

where $\bar{U}_r^{(\max)} = \bar{U}_r^{(s)}(r = r_{\max}, z \rightarrow 0)$ and r_{\max} is the radius at which the function $J_1(Y)$ reaches the maximum value. In Fig. 10 we show the radial profiles of the ratios L_O/L_z and $u_*/\bar{U}_r^{(\max)}$, which demonstrate that these ratios are small.

V. CONCLUSIONS

In the present study we investigate essential features of turbulence and semi-organised structures in the core of the atmospheric convective boundary-layer (the CBL core) by means of the energy- and flux budget (EFB) theory. We find the global turbulent characteristics (averaged over the entire volume of the semi-organised structure) including turbulent kinetic energy and intensity of

potential temperature fluctuations, turbulent flux of potential temperature, as well as the kinetic and thermal energies of the semi-organised structures. These characteristics depend on the aspect ratio of the semi-organised structure and the scale separation parameter between the vertical size of the structures and the integral scale of turbulence.

We demonstrate that when plumes are extended in the vertical direction ($\ell_h^{(pl)}/\ell_z^{(pl)} < 1$), the vertical turbulent flux of potential temperature averaged over the entire volume of the semi-organised structure $\langle F_z \rangle_V$ is negative (see Fig. 2), where $\ell_h^{(pl)}$ and $\ell_z^{(pl)}$ are the horizontal and vertical scales in which the two-point instantaneous correlation functions $\langle \theta(t, \mathbf{x}) u_z(t, \mathbf{x} + \mathbf{r}) \rangle$ characterised the plumes, vanish in the horizontal and vertical directions, respectively. In this case, the mean vertical gradient of the potential temperature $\nabla_z \bar{\Theta}^{(m)}$ can be positive inside the semi-organised structure [see Eq. (45) and Fig. 9]. On the other hand, the vertical flux of potential temperature $\langle \bar{\Theta}^{(s)} \bar{U}_z^{(s)} \rangle_V$ transported by the semi-organised structures is much larger than the vertical turbulent flux $\langle F_z \rangle_V$ of potential temperature [see Eq. (38) and Fig. 7].

The turbulent kinetic energy density $\langle E_K \rangle_V$ is much smaller than the kinetic energy density of semi-organised structures $\langle E_U \rangle_V$ [see Eq. (36) and Fig. 6]. Increase of the scale separation between the vertical size L_z of the semi-organised structures and the vertical integral scale of turbulence ℓ_z , increases the kinetic energy density $\langle E_U \rangle_V$ of the semi-organised structures and the ratio $\langle E_U \rangle_V / \langle E_K \rangle_V$. Similarly, the turbulent thermal energy $\langle E_\theta \rangle_V$ is much smaller than the thermal energy of the semi-organised structures $\langle E_\Theta \rangle_V$ [see Eq. (40) and Fig. 8].

We perform matching between the solutions obtained for the CBL core and the convective surface layer. This yields the ratio of the local Obukhov length scale, $L_O = -u_*^3/(\beta \tilde{F}_z)$, for the convective surface layer to the vertical size of the semi-organised structure L_z as well as the ratio of the friction velocity u_* to the maximum value of the horizontal velocity of the semi-organized structure $\bar{U}_r^{(s)}$ [see Eqs. (54) and (56), as well as Fig. 10]. The obtained theoretical results are important for modelling applications in the atmospheric convective boundary-layer.

DEDICATION

This paper was dedicated to Prof. Sergej Zilitinkevich (1936-2021) who initiated this work and discussed some of the obtained results.

ACKNOWLEDGMENTS

This research was supported in part by the PAZY Foundation of the Israel Atomic Energy Commission (grant No. 122-2020).

AUTHOR DECLARATIONS

Conflict of Interest

The authors have no conflicts to disclose.

DATA AVAILABILITY

Data sharing is not applicable to this article as no new data were created or analyzed in this study.

Appendix A: Functions $f(A_*)$

$$f_{\hat{F}}(A_*) = \frac{(2\pi)^2}{3} \frac{(1 + A_*^2)^2}{A_*^2 \sigma (A_*^2 - \mu)}, \quad (\text{A1})$$

$$\tilde{f}_S(A_*) = \lambda^2 J_0^2(\lambda) (1 + A_*^2)^2 + 2A_*^2 [J_0^2(\lambda) - 1], \quad (\text{A2})$$

$$f_S(A_*) = \left(\frac{\pi}{\lambda A_*} \right)^2 \tilde{f}_S(A_*), \quad (\text{A3})$$

$$f_{F_s}(A_*) = \frac{\pi^2}{\sqrt{3}} J_0^2(\lambda) \frac{(1 + A_*^2)^2}{A_*^2} f_S^{1/2}(A_*), \quad (\text{A4})$$

$$f_U(A_*) = \frac{J_0^2(\lambda)}{4} \frac{(1 + A_*^2)}{f_{F_s}^{2/3}(A_*)}, \quad (\text{A5})$$

$$f_\Theta(A_*) = \frac{f_{F_s}^{2/3}(A_*)}{J_0^2(\lambda)}, \quad (\text{A6})$$

$$f_u(A_*) = \frac{f_S(A_*)}{f_{F_s}^{2/3}(A_*)}, \quad (\text{A7})$$

$$f_{F_T}(A_*) = \frac{1}{\sqrt{3}} \frac{f_{\hat{F}}(A_*) f_S^{3/2}(A_*)}{f_{F_s}(A_*)}, \quad (\text{A8})$$

$$f_\theta(A_*) = 8\pi^2 \frac{1 + A_*^2}{A_*^2} f_\Theta(A_*), \quad (\text{A9})$$

$$f_D(A_*) = 2\sqrt{3} \frac{f_\theta(A_*)}{f_{F_T}(A_*) f_u^{1/2}(A_*)}, \quad (\text{A10})$$

$$f_\nabla(A_*) = \frac{f_{F_T}(A_*)}{2\sqrt{3} f_u^{1/2}(A_*)}. \quad (\text{A11})$$

Appendix B: Identities used for derivation of Eqs. (27), (29), (34), (39) and (43)

To derive Eq. (27), we use the following equations:

$$\left\langle \left(\nabla_r \bar{U}_r^{(s)} \right)^2 \right\rangle_v = \frac{1}{2} \left(\frac{\bar{U}_{z0}}{R} \right)^2 A_*^2 [(1 + \lambda^2) J_0^2(\lambda) - 1], \quad (\text{B1})$$

$$\begin{aligned} \left\langle \left(\nabla_z \bar{U}_z^{(s)} \right)^2 \right\rangle_v &= - \left\langle \left(\nabla_r \bar{U}_z^{(s)} \right) \left(\nabla_z \bar{U}_r^{(s)} \right) \right\rangle_v \\ &= \frac{1}{2} \left(\frac{\bar{U}_{z0}}{R} \right)^2 A_*^2 \lambda^2 J_0^2(\lambda), \end{aligned} \quad (\text{B2})$$

$$\left\langle \left(\nabla_z \bar{U}_r^{(s)} \right)^2 \right\rangle_v = \frac{1}{2} \left(\frac{\bar{U}_{z0}}{R} \right)^2 A_*^4 \lambda^2 J_0^2(\lambda), \quad (\text{B3})$$

$$\left\langle \left(\nabla_r \bar{U}_z^{(s)} \right)^2 \right\rangle_v = \frac{1}{2} \left(\frac{\bar{U}_{z0}}{R} \right)^2 \lambda^2 J_0^2(\lambda), \quad (\text{B4})$$

where we use integrals given by Eqs. (B14)–(B15).

To derive Eq. (29), we use the following equation:

$$\left\langle \bar{\Theta}^{(s)} \bar{U}_z^{(s)} \right\rangle_v = \frac{1}{2} \bar{\Theta}_0 \bar{U}_{z0} J_0^2(\lambda), \quad (\text{B5})$$

where we use integrals given by Eq. (B14). To derive Eq. (33), we use the following equation:

$$\begin{aligned} \left\langle \left(\bar{U}_z^{(s)} \right)^2 \right\rangle_v &= A_*^{-2} \left\langle \left(\bar{U}_r^{(s)} \right)^2 \right\rangle_v \\ &= \frac{\bar{U}_{z0}^2}{2} J_0^2(\lambda), \end{aligned} \quad (\text{B6})$$

where we use integrals given by Eq. (B14). To derive Eq. (34), we use the following equation:

$$\left\langle \left(\bar{\Theta}^{(s)} \right)^2 \right\rangle_v = \bar{\Theta}_0^2 \frac{J_0^2(\lambda)}{2}, \quad (\text{B7})$$

where we use integrals given by Eq. (B14).

To derive Eq. (39) for the turbulent thermal energy $\langle E_\theta \rangle_v$ in a convective turbulence, we use budget equations (15)–(16) for E_θ and F_i in a steady-state for homogeneous turbulent convection:

$$\begin{aligned} F_z &= 2C_F t_T \left[C_\theta \beta E_\theta - E_z \nabla_z \left(\bar{\Theta}^{(m)} + \bar{\Theta}^{(s)} \right) \right. \\ &\quad \left. - \frac{1}{2} F_r \left(\nabla_r \bar{U}_z^{(s)} \right) \right], \end{aligned} \quad (\text{B8})$$

$$F_r = -2C_F t_T E_r \nabla_r \bar{\Theta}^{(s)}, \quad (\text{B9})$$

$$E_\theta = -2C_P t_T \left[(\mathbf{F} \cdot \nabla) \bar{\Theta}^{(s)} + F_z \nabla_z \bar{\Theta}^{(m)} \right]. \quad (\text{B10})$$

Using Eq. (B8), we determine $\left\langle (F_z \nabla_z) \bar{\Theta}^{(s)} \right\rangle_v$. Substituting the obtained expression into Eq. (B10) averaged over the organised-structure volume, we obtain expression for the turbulent thermal energy $\langle E_\theta \rangle_v$ as

$$\begin{aligned} \langle E_\theta \rangle_v &= 4C_P C_F \ell^2 \left[A_z \left\langle \left(\nabla_z \bar{\Theta}^{(s)} \right)^2 \right\rangle_v \right. \\ &\quad \left. + A_r \left\langle \left(\nabla_r \bar{\Theta}^{(s)} \right)^2 \right\rangle_v \right], \end{aligned} \quad (\text{B11})$$

where $A_r = E_r/E_K = A_z = 1/3$ is the horizontal anisotropy parameter and

$$\begin{aligned} \left\langle \left(\nabla_z \bar{\Theta}^{(s)} \right)^2 \right\rangle_v &= A_*^2 \left\langle \left(\nabla_r \bar{\Theta}^{(s)} \right)^2 \right\rangle_v \\ &= \frac{\pi^2}{2} \left(\frac{\Theta_0}{L_z} \right)^2 J_0^2(\lambda). \end{aligned} \quad (\text{B12})$$

To derive Eq. (B12), we use integrals given by Eq. (B14). Substituting Eq. (B12) into Eq. (B11), we obtain the turbulent thermal energy $\langle E_\theta \rangle_v$ given by Eq. (39).

To derive Eq. (43), we use the following equation:

$$\begin{aligned} \left\langle \left(\nabla_r \bar{\Theta}^{(s)} \right) \left(\nabla_r \bar{U}_z^{(s)} \right) \right\rangle_v &= \frac{\lambda^2}{2R^2} \bar{\Theta}_0 \bar{U}_{z0} J_0^2(\lambda) \\ &= \frac{\pi^2}{L_z^2 A_*^2} \Theta_D U_D, \end{aligned} \quad (\text{B13})$$

where we use integrals given by Eq. (B14).

For the derivation of equations in this Appendix, we used the following integrals:

$$\begin{aligned} \int_0^1 X J_0^2(\lambda X) dX &= \int_0^1 X J_1^2(\lambda X) dX \\ &= \int_0^1 X J_2^2(\lambda X) dX = \frac{1}{2} J_0^2(\lambda) = \frac{1}{2} J_2^2(\lambda), \end{aligned} \quad (\text{B14})$$

$$\int_0^1 X J_0(\lambda X) J_2(\lambda X) dX = \frac{1}{\lambda^2} \left[1 - \left(1 + \frac{1}{2} \lambda^2 \right) J_0^2(\lambda) \right]. \quad (\text{B15})$$

$$\int_0^1 J_0(\lambda X) J_1(\lambda X) dX = \frac{1}{2\lambda} \left[1 - J_0^2(\lambda) \right], \quad (\text{B16})$$

-
- [1] A. S. Monin and A. M. Yaglom, *Statistical Fluid Mechanics*, Vol. 1 (MIT Press, 1971).
 - [2] A. S. Monin and A. M. Yaglom, *Statistical Fluid Mechanics*, Vol. 2 (Courier Corporation, 2013).
 - [3] W. D. McComb, *The Physics of Fluid Turbulence* (Oxford Science Publications, 1990).
 - [4] U. Frisch, *Turbulence: the Legacy of A. N. Kolmogorov* (Cambridge University Press, Cambridge, 1995).
 - [5] S. B. Pope, *Turbulent Flows* (Cambridge University Press, Cambridge, 2000).
 - [6] M. Lesieur, *Turbulence in Fluids* (Springer, 2008).
 - [7] P. Sagaut and C. Cambon, *Homogeneous turbulence dynamics*, Vol. 10 (Springer, 2008).
 - [8] S. S. Zilitinkevich, *Turbulent Penetrative Convection* (Aldershot: Avebury Technical, 1991).
 - [9] J. C. Kaimal and J. J. Finnigan, *Atmospheric Boundary Layer Flows: Their Structure and Measurement* (Oxford University press, 1994).
 - [10] P. A. Davidson, *Turbulence in Rotating, Stratified and Electrically Conducting Fluids* (Cambridge University Press, Cambridge, 2013).
 - [11] I. Rogachevskii, *Introduction to Turbulent Transport of Particles, Temperature and Magnetic Fields* (Cambridge University Press, Cambridge, 2021).
 - [12] A. N. Kolmogorov, Dissipation of energy in the locally isotropic turbulence, *Dokl. Akad. Nauk SSSR A* **32**, 16 (1941).
 - [13] A. N. Kolmogorov, Energy dissipation in locally isotropic turbulence, *Dokl. Akad. Nauk. SSSR A* **32**, 19 (1941).
 - [14] A. N. Kolmogorov, The local structure of turbulence in incompressible viscous fluid for very large reynolds numbers, *Proc. Roy. Soc. London A* **434**, 9 (1991).
 - [15] A. N. Kolmogorov, The equations of turbulent motion in an incompressible fluid, *Izvestia Akad. Sci., USSR; Phys.* **6**, 56 (1942).
 - [16] J. Kondo, O. Kanechika, and N. Yasuda, Heat and momentum transfers under strong stability in the atmospheric surface layer, *J. Atmosph. Sci.* **35**, 1012 (1978).
 - [17] F. Bertin, J. Barat, and R. Wilson, Energy dissipation rates, eddy diffusivity, and the prandtl number: An in situ experimental approach and its consequences on radar estimate of turbulent parameters, *Radio Science* **32**, 791 (1997).
 - [18] Y. Ohya, Wind-tunnel study of atmospheric stable boundary layers over a rough surface, *Boundary-Layer Meteorol.* **98**, 57 (2001).
 - [19] E. J. Strang and H. J. S. Fernando, Vertical mixing and transports through a stratified shear layer, *J. Phys. Oceanogr.* **31**, 2026 (2001).
 - [20] C. R. Rehmann and J. R. Koseff, Mean potential energy change in stratified grid turbulence, *Dynamics of Atmospheres and Oceans* **37**, 271 (2004).
 - [21] L. Mahrt and D. Vickers, Boundary-layer adjustment over small-scale changes of surface heat flux, *Boundary-Layer Meteorology* **116**, 313 (2005).
 - [22] D. D. Stretch, J. W. Rottman, S. K. Venayagamoorthy, K. K. Nomura, and C. R. Rehmann, Mixing efficiency in decaying stably stratified turbulence, *Dynamics of Atmospheres and Oceans* **49**, 25 (2010).
 - [23] L. Mahrt, Variability and maintenance of turbulence in the very stable boundary layer, *Boundary-Layer Meteorology* **135**, 1 (2010).
 - [24] S. S. Zilitinkevich, T. Elperin, N. Kleeorin, I. Rogachevskii, and I. Esau, A hierarchy of energy- and flux-budget (EFB) turbulence closure models for stably stratified geophysical flows, *Boundary-Layer Meteorol.* **146**, 341 (2013).
 - [25] L. Mahrt, Stably stratified atmospheric boundary layers, *Annual Review of Fluid Mechanics* **46**, 23 (2014).
 - [26] D. Li, G. G. Katul, and S. S. Zilitinkevich, Closure schemes for stably stratified atmospheric flows without turbulence cutoff, *J. Atmosph. Sci.* **73**, 4817 (2016).
 - [27] D. Li, Turbulent Prandtl number in the atmospheric boundary layer – Where are we now?, *Atmosph. Res.* **216**, 86 (2019).
 - [28] S. S. Zilitinkevich, Turbulence and diffusion in free convection, *Izv. Acad. Sci. USSR Atmos. Ocean. Phys.* **7**, 825 (1971).
 - [29] S. S. Zilitinkevich, Shear convection, *Boundary-Layer Meteor.*, **3**, 416 (1973).
 - [30] B. Kader and A. Yaglom, Mean fields and fluctuation moments in unstably stratified turbulent boundary layers, *J. Fluid Mech.* **212**, 637 (1990).
 - [31] S. Zilitinkevich, E. Kadantsev, I. Repina, E. Mortikov, and A. Glazunov, Order out of chaos: Shifting paradigm of convective turbulence, *J. Atmosph. Sci.* **78**, 3925 (2021).
 - [32] H. Schmidt and U. Schumann, Coherent structure of the convective boundary layer derived from large-eddy simulations, *Journal of Fluid Mechanics* **200**, 511 (1989).
 - [33] R. I. Sykes and D. S. Henn, Large-eddy simulation of turbulent sheared convection, *J. Atmosph. Sci.* **46**, 1106 (1989).
 - [34] L. Mahrt, Eddy asymmetry in the sheared heated boundary layer, *J. Atmosph. Sci.* **48**, 472 (1991).
 - [35] A. G. Williams and J. M. Hacker, The composite shape and structure of coherent eddies in the convective boundary layer, *Boundary-Layer Meteorology* **61**, 213 (1992).
 - [36] A. G. Williams and J. M. Hacker, Interactions between coherent eddies in the lower convective boundary layer, *Boundary-Layer Meteorology* **64**, 55 (1993).
 - [37] S. Zilitinkevich, J. Hunt, I. N. Esau, A. Grachev, D. Lalas, E. Akylas, M. Tombrou, C. Fairall, H. Fernando, A. Baklanov, *et al.*, The influence of large convective eddies on the surface-layer turbulence, *Quart. J. Roy. Meteorolog. Soc.* **132**, 1426 (2006).
 - [38] T. Elperin, N. Kleeorin, I. Rogachevskii, and S. Zilitinkevich, Formation of large-scale semi-organized structures in turbulent convection, *Phys. Rev. E* **66**, 066305 (2002).
 - [39] T. Elperin, N. Kleeorin, I. Rogachevskii, and S. Zilitinkevich, Tangling turbulence and semi-organized structures in convective boundary layers, *Boundary-Layer Meteorol.* **119**, 449 (2006).
 - [40] A. Hellsten and S. Zilitinkevich, Role of convective structures and background turbulence in the dry convective boundary layer, *Boundary-Layer Meteorology* **149**, 323 (2013).
 - [41] D. Etling and R. A. Brown, Roll vortices in the planetary boundary layer: A review, *Boundary-Layer Meteorol.* **65**, 215 (1993).
 - [42] B. W. Atkinson and J. Wu Zhang, Mesoscale shallow convection in the atmosphere, *Rev. Geophys.* **34**, 403 (1996).

- [43] B. Brümmer, Roll and cell convection in wintertime arctic cold-air outbreaks, *J. Atmosph. Sci.* **56**, 2613 (1999).
- [44] S. S. Zilitinkevich, T. Elperin, N. Kleeorin, V. L'vov, and I. Rogachevskii, Energy-and flux-budget turbulence closure model for stably stratified flows. Part II: The role of internal gravity waves, *Boundary-Layer Meteorol.* **133**, 139 (2009).
- [45] N. Kleeorin, I. Rogachevskii, I. A. Soustova, Y. I. Troitskaya, O. S. Ermakova, and S. Zilitinkevich, Internal gravity waves in the energy and flux budget turbulence-closure theory for shear-free stably stratified flows, *Phys. Rev. E* **99**, 063106 (2019).
- [46] A. M. Yaglom, Fluctuation spectra and variances in convective turbulent boundary layers: A reevaluation of old models, *Physics of Fluids* **6**, 962 (1994).
- [47] J. Wyngaard and O. Coté, The budgets of turbulent kinetic energy and temperature variance in the atmospheric surface layer, *J. Atmosph. Sci.* **28**, 190 (1971).
- [48] V. Canuto and F. Minotti, Stratified turbulence in the atmosphere and oceans: A new subgrid model, *J. Atmosph. Sci.* **50**, 1925 (1993).
- [49] T. Elperin, I. Golubev, N. Kleeorin, and I. Rogachevskii, Large-scale instabilities in a nonrotating turbulent convection, *Phys. Fluids* **18**, 126601 (2006).
- [50] V. M. Canuto, Turbulence in astrophysical and geophysical flows, in *Interdisciplinary aspects of turbulence* (Springer, 2008) pp. 107–160.
- [51] A. Glazunov and V. Dymnikov, Spatial spectra and characteristic horizontal scales of temperature and velocity fluctuations in the convective boundary layer of the atmosphere, *Izv. Atmos. Ocean. Phys.* **49**, 33 (2013).
- [52] T. Banerjee, G. Katul, S. Salesky, and M. Chamecki, Revisiting the formulations for the longitudinal velocity variance in the unstable atmospheric surface layer, *Quart. J. Roy. Meteorolog. Soc.* **141**, 1699 (2015).
- [53] S. T. Salesky, M. Chamecki, and E. Bou-Zeid, On the nature of the transition between roll and cellular organization in the convective boundary layer, *Boundary-Layer Meteorol.* **163**, 41 (2017).
- [54] S. Salesky and W. Anderson, Buoyancy effects on large-scale motions in convective atmospheric boundary layers: implications for modulation of near-wall processes, *J. Fluid Mech.* **856**, 135 (2018).
- [55] S. Salesky and W. Anderson, Coherent structures modulate atmospheric surface layer flux-gradient relationships, *Phys. Rev. Lett.* **125**, 124501 (2020).
- [56] B. Kader and A. Yaglom, Spectra and correlation functions of surface layer atmospheric turbulence in unstable thermal stratification, in *Turbulence and coherent structures* (Springer, 1991) pp. 387–412.
- [57] J. Sun, D. H. Lenschow, M. A. LeMone, and L. Mahrt, The role of large-coherent-eddy transport in the atmospheric surface layer based on cases-99 observations, *Boundary-Layer Meteorology* **160**, 83 (2016).
- [58] A. A. Grachev, P. O. G. Persson, T. Uttal, E. A. Akish, C. J. Cox, S. M. Morris, C. W. Fairall, R. S. Stone, G. Lesins, A. P. Makshtas, *et al.*, Seasonal and latitudinal variations of surface fluxes at two arctic terrestrial sites, *Climate Dynamics* **51**, 1793 (2018).
- [59] J. Garratt, *The atmospheric boundary layer* (Cambridge Univ. Press, 1992).
- [60] J. C. Wyngaard, *Turbulence in the Atmosphere* (Cambridge University Press, 2010).
- [61] F. Tampieri, *Turbulence and dispersion in the planetary boundary layer* (Springer, 2017).
- [62] U. Schumann, Minimum friction velocity and heat transfer in the rough surface layer of a convective boundary layer, *Boundary-Layer Meteorology* **44**, 311 (1988).
- [63] R. I. Sykes, D. S. Henn, and W. S. Lewellen, Surface-layer description under free-convection conditions, *Quart. J. Royal Meteorol. Soc.* **119**, 409 (1993).
- [64] S. Zilitinkevich, V. M. Gryanik, V. N. Lykossov, and D. V. Mironov, Third-order transport and nonlocal turbulence closures for convective boundary layers, *J. Atmosph. Sci.* **56**, 3463 (1999).
- [65] S. S. Zilitinkevich, T. Elperin, N. Kleeorin, and I. Rogachevskii, Energy- and flux budget (EFB) turbulence closure model for stably stratified flows. Part I: Steady-state, homogeneous regimes, *Boundary-Layer Meteorol.* **125**, 167 (2007).
- [66] S. S. Zilitinkevich, T. Elperin, N. Kleeorin, I. Rogachevskii, I. Esau, T. Mauritsen, and M. W. Miles, Turbulence energetics in stably stratified geophysical flows: Strong and weak mixing regimes, *Quarterly J. Roy. Meteorol. Soc.* **134**, 793 (2008).
- [67] S. S. Zilitinkevich, I. Esau, N. Kleeorin, I. Rogachevskii, and R. D. Kouznetsov, On the velocity gradient in stably stratified sheared flows. Part 1: Asymptotic analysis and applications, *Boundary-Layer Meteorol.* **135**, 505 (2010).
- [68] N. Kleeorin, I. Rogachevskii, and S. Zilitinkevich, Energy and flux budget closure theory for passive scalar in stably stratified turbulence, *Phys. Fluids* **33**, 076601 (2021).
- [69] I. Rogachevskii, N. Kleeorin, and S. Zilitinkevich, Energy-and flux-budget theory for surface layers in atmospheric convective turbulence, *Phys. Fluids* **34** (2022).
- [70] Y. Cheng, V. Canuto, A. Howard, A. Ackerman, M. Kelley, A. Fridlind, G. Schmidt, M. Yao, A. Del Genio, and G. Elsaesser, A second-order closure turbulence model: new heat flux equations and no critical richardson number, *J. Atmosph. Sci.* **77**, 2743 (2020).
- [71] G. Orian, A. Asulin, E. Tkachenko, N. Kleeorin, A. Levy, and I. Rogachevskii, Large-scale circulations in a shear-free convective turbulence: Mean-field simulations, *Phys. Fluids* **34** (2022).
- [72] L. Ostrovsky and Y. I. Troitskaya, A model of turbulent transfer and dynamics of turbulence in a stratified shear-flow, *Izv. Atmos. Ocean. Phys.* **23**, 1031 (1987).
- [73] V. Canuto, Y. Cheng, A. Howard, and I. Esau, Stably stratified flows: A model with no ri (cr), *J. Atmosph. Sci.* **65**, 2437 (2008).
- [74] V. S. L'vov, I. Procaccia, and O. Rudenko, Energy conservation and second-order statistics in stably stratified turbulent boundary layers, *Environmental Fluid Mechanics* **9**, 267 (2009).
- [75] I. Esau, Simulation of ekman boundary layers by large eddy model with dynamic mixed subfilter closure, *Environmental Fluid Mech.* **4**, 273 (2004).
- [76] I. N. Esau and S. S. Zilitinkevich, Universal dependences between turbulent and mean flow parameters instably and neutrally stratified planetary boundary layers, *Nonlinear Processes in Geophysics* **13**, 135 (2006).
- [77] J. L. Lumley, Rational approach to relations between motions of differing scales in turbulent flows, *Phys. Fluids* **10**, 1405 (1967).
- [78] J. C. Wyngaard and O. R. Coté, Cospectral similarity in the atmospheric surface layer, *Quarterly Journal of the Royal Meteorological Society* **98**, 590 (1972).
- [79] S. G. Saddoughi and S. V. Veeravalli, Local isotropy in

- turbulent boundary layers at high reynolds number, *Journal of Fluid Mechanics* **268**, 333 (1994).
- [80] T. Ishihara, K. Yoshida, and Y. Kaneda, Anisotropic velocity correlation spectrum at small scales in a homogeneous turbulent shear flow, *Physical Review Letters* **88**, 154501 (2002).
 - [81] J. Niemela, L. Skrbek, K. Sreenivasan, and R. Donnelly, The wind in confined thermal convection, *J. Fluid Mech.* **449**, 169 (2001).
 - [82] L. Barel, A. Eidelman, T. Elperin, G. Fleurov, N. Kleeorin, A. Levy, I. Rogachevskii, and O. Shildkrot, Detection of standing internal gravity waves in experiments with convection over a wavy heated wall, *Phys. Fluids* **32** (2020).
 - [83] A. Brandenburg, Stellar mixing length theory with entropy rain, *Astrophys. J.* **832**, 6 (2016).
 - [84] P. J. Käpylä, M. Rheinhardt, A. Brandenburg, R. Arlt, M. J. Käpylä, A. Lagg, N. Olsper, and J. Warnecke, Extended subadiabatic layer in simulations of overshooting convection, *Astrophys. J. Lett.* **845**, L23 (2017).
 - [85] P. J. Käpylä, Overshooting in simulations of compressible convection, *Astron. Astrophys.* **631**, A122 (2019).
 - [86] S. Toppaladoddi, S. Succi, and J. S. Wettlaufer, Roughness as a route to the ultimate regime of thermal convection, *Phys. Rev. Lett.* **118**, 074503 (2017).